

## Reproducibility of Mode Transition of Edge Tone with DNS and LES

Sho IWAGAMI<sup>(1)</sup>, Taizo KOBAYASHI<sup>(2)</sup>, Kin'ya TAKAHASHI<sup>(3)</sup>, Yuji Hattori<sup>(4)</sup>

<sup>(1)</sup>Kyushu Institute of Technology, Japan, iwagami@chaos.mse.kyutech.ac.jp

<sup>(2)</sup>Kyushu University, Japan, tkoba@cc.kyushu-u.ac.jp

<sup>(3)</sup>Kyushu Institute of Technology, Japan, takahasi@mse.kyutech.ac.jp

<sup>(4)</sup>Tohoku University, Japan, hattori@fmail.ifs.tohoku.ac.jp

### Abstract

A jet attacking a edge oscillates spontaneously, and generates aerodynamic sound called edge tone. The edge tone is the sound source of air-jet instruments like a recorder and flute. The jet oscillation has several modes. While one of the modes is selected, the frequency increases linearly with the jet velocity. When the jet velocity exceeds a threshold, the mode transition arises, and it is hysteretic. The mode transition induces sudden changes of the frequency and the sound energy. Therefore, the reproducibility of the mode transition with a numerical calculation is crucial for understanding the mechanism of edge tone. In this study, the 2D model of edge tone is investigated with compressible DNS and LES. The DNS adopted in our study is an exact method without any artificial viscosity terms. The mode transition can be accurately reproduced with DNS. On the other hand, in some cases of calculations with LES, the mode transition cannot be reproduced even though the calculation is not broken down. We discuss the details of this problem.

Keywords: Aerodynamic Sound, Edge tone, DNS, LES

## 1 INTRODUCTION

Edge tone is generated from oscillating jet colliding with an edge and is one of the aerodynamic sounds observed in a low Mach number region. The study of the sounding mechanism of edge tone is a long standing problem in the field of aeroacoustics as well as musical acoustics[1, 2]. That is, it is the sound source of air-jet instruments and the study of edge tone leads us to understand the sound mechanism of air-jet instruments.

In the long history of study of the edge tone, some phenomenological formulas which describe the relation between the edge tone frequency and the jet velocity have been proposed [1, 3, 4, 5, 6]. A very useful formula introduced by Brown [3] based on experimental results shows that the frequency of the edge tone increases in proportion to the jet velocity until a mode transition arises. At the mode transition, the hydrodynamic wave of the jet jump to a higher mode and the change of the tone is observed. However, the transition mechanism between the hydrodynamics modes is not theoretically elucidated yet.

As an alternative approach, we can rely on numerical methods of the compressible fluid to reproduce hydrodynamic and acoustic motions simultaneously. In this paper, we treat two numerical methods, compressible Direct Numerical Simulation (DNS) and compressible Large Eddy Simulation (LES). Our compressible DNS dose not include any artificial viscosity terms and is considered as the most reliable scheme. First, we investigate how accurately the hydrodynamic mode transition of edge tone is reproduced with DNS. We treat a 2D model of edge tone, because DNS requires a huge computer power, and find that it well reproduces the hydrodynamic mode transition. Next, we treat LES as a practical scheme for the calculations of 2D and 3D models and investigate the reliability of LES with changing grid interval taking DNS as a reference.

## 2 HYSTERETIC MODE TRANDITION OF EDGE TONE

As shown in Fig.1, a jet injected from a flue collides with an edge and causes vortices. The reaction of vortices influences the jet to oscillate in the vertical direction. The aerodynamic sound, known as edge tone, is created

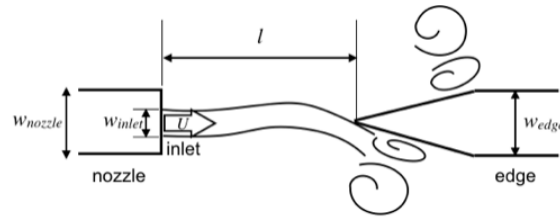


Figure 1. Edge tone : In the 2D model, the parameters are taken as  $l = 5\text{mm}$ ,  $w_{edge} = 1.2\text{mm}$ ,  $w_{nozzle} = 1.2$ ,  $w_{inlet} = 1\text{mm}$ .

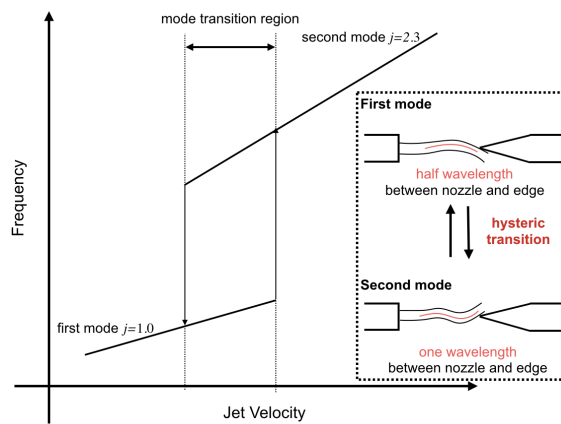


Figure 2. Hysteretic mode transition of edge tone.

by the oscillating jet together with the vortices [1].

The relation between the oscillation frequency of the edge tone and the jet velocity is given by Brown's equation [3],

$$f = 0.466j(100U - 40)(1/(100l) - 0.07), \quad (1)$$

where  $f$ [Hz],  $U$ [m/s] and  $l$ [m] are the oscillation frequency, jet velocity and distance between the flue exit and the edge, respectively. The parameter  $j$  changes with the oscillation mode of the jet and has values  $j = 1.0, 2.3, 3.8$  and  $5.4$ . The value  $j = 1$  corresponds to the first hydrodynamic mode and other values correspond to higher hydrodynamic modes. The frequency of the first mode increases linearly with increasing  $U$ . But an oscillation jumps to one of the higher modes if  $U$  exceeds its threshold value. As shown in Fig.2, the transition is hysteretic, namely the downward transition occurs a different threshold value, which is less than that of the upward transition. Let us call the region between these threshold values the hysteretic transition region from  $U=12\text{m/s}$  to  $17.5\text{m/s}$ .

### 3 NUMERICAL MODEL AND METHOD

Figure.1 shows a 2D model of the edge tone studied in this paper, where  $l = 5\text{mm}$ . According to Brown's experiment[3], at  $l = 5\text{mm}$  the transition region is located from  $U=12\text{m/s}$  to  $17.5\text{m/s}$ . The velocity distribution at the inlet is given by the Hagen-Poiseuille flow and  $U$  denotes the mean velocity at the inlet.

In this paper, we use two numerical methods, DNS and LES, for calculating the edge tone. The compressible DNS we use in this paper is the most reliable scheme without any artificial viscosity terms[7].

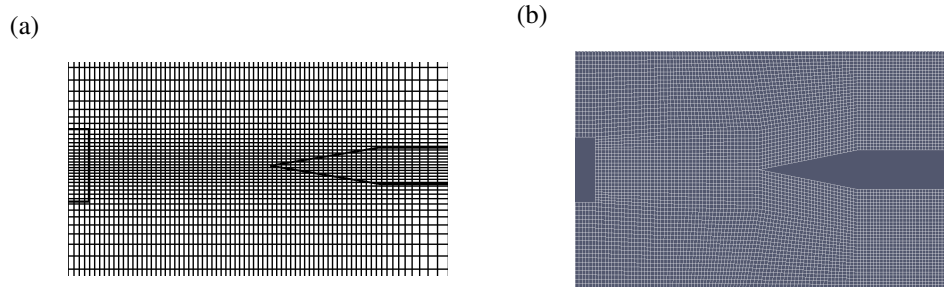


Figure 3. Mesh of DNS and LES : (a) DNS mesh at  $U=3.3\text{m/s}$ . The lines are drawn every 10 grid intervals. (b) LES mesh with  $x_{min} = 0.1\text{mm}$ .

The volume penalization (VP) method, which is one of the immersed boundary methods, has been applied mostly to incompressible flows. In the VP method we solve the Navier-Stokes equations supplemented by penalization terms instead of imposing no-slip boundary conditions at the surface of rigid bodies in the flow. Actually, the sixth-order-accurate compact scheme is used except that the fourth-order central scheme is used for the penalization terms; for time evolution the second-order implicit method is used for the penalization terms, while the second-order Adams-Bashforth method is used for the other terms. Figure.3 (a) shows a mesh of DNS at  $U = 3.3\text{m/s}$  with time step  $\Delta t = 1.8 \times 10^{-9}\text{s}$ . To reproduce the whole behavior of the compressible fluid including acoustic waves, the minimum grid scale  $\Delta x_{min}$  should be set in a viscous subrange of energy cascade:  $\Delta x_{min} = 6.4\mu\text{m}$ . The minimum grid scale  $\Delta x_{min}$  decreases with increasing  $U$ . For example,  $\Delta x_{min} = 2.5\mu\text{m}$  at  $U = 20\text{m/s}$  with time step  $\Delta t = 1.2 \times 10^{-9}\text{s}$ .

Although, our compressible DNS is a very accurate scheme, it requires huge computer resources even for 2D calculations. A compressible LES is often used as a realistic method for the calculations of 2D and 3D models of musical instruments[8, 9]. In this paper, we investigate the reliability of compressible LES taking DNS as a reference. We use a compressible LES solver in the open source software, OpenFOAM ver.5.0. Specifically, we use scheme called “rhoPimpleFoam” with the one-equation sub-grid-scale(SGS) model, which is suitable for fluid at subsonic speeds. We study two mesh models : the coarse grained mesh with  $\Delta x_{min} = 0.1\text{mm}$ ,  $\Delta t = 1.0 \times 10^{-7}$  and the fine grained mesh with  $\Delta x_{min} = 0.05\text{mm}$ ,  $\Delta t = 5.0 \times 10^{-8}$ . Figure.3 (b) showed the coarse grained mesh.

## 4 NUMERICAL RESULTS

### 4.1 DNS Results

By using DNS, we simulated the edge tone at some representative values of  $U$  in a range (3.3, 20.0) in units of millimeter. Figure.4 (a) and (b) show velocity distribution and pressure distribution at  $U = 4.7\text{m/s}$ , respectively. Figure.5 (a) and (b) show those at  $U = 18.3\text{m/s}$ . In Fig.4 (a), the hydrodynamic oscillation of the fundamental mode is observed, while in Fig.5 (a), that of the second mode is observed. As shown in Fig.4 (b), the upper and lower distributions in pressure seem to oscillate in anti-phase to each other. Namely, anti-phase acoustic waves are radiated to the upper and lower sides. This means that the oscillating jet behaves like a dipole source. As shown in Fig.5 (b), the dipole radiation is also observed in the second mode.

Fig.6 shows the change of the sound frequency with the jet velocity  $U$  compared with Brown’s equation (1). Below the hysteretic transition region the sound frequencies follow the first mode of Brown’s equation, while above the transition region they follow the second mode. In the transition region, the oscillations fall into either the first mode or the second mode, and which mode to be selected sensitively depends on a tiny initial noise, which is added to break the upper and lower symmetry of the flow and to induce the jet oscillation.

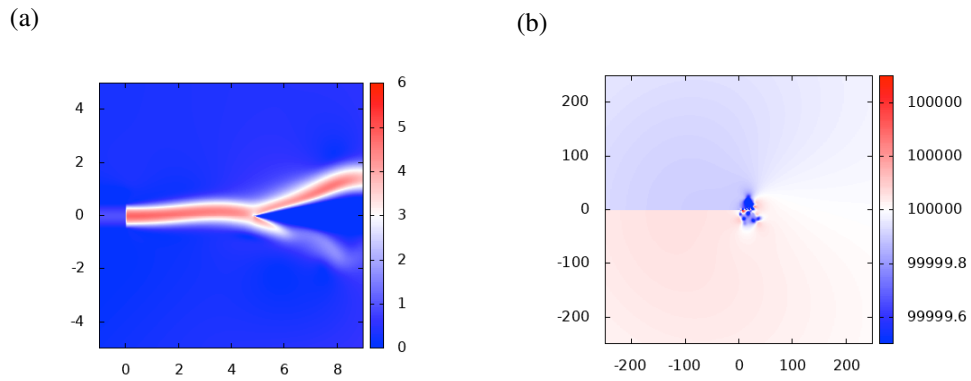


Figure 4. Result of DNS at  $U=4.7\text{m/s}$ . The unit of the horizontal and vertical axes is mm. (a) Velocity distribution. (b) Pressure distribution.

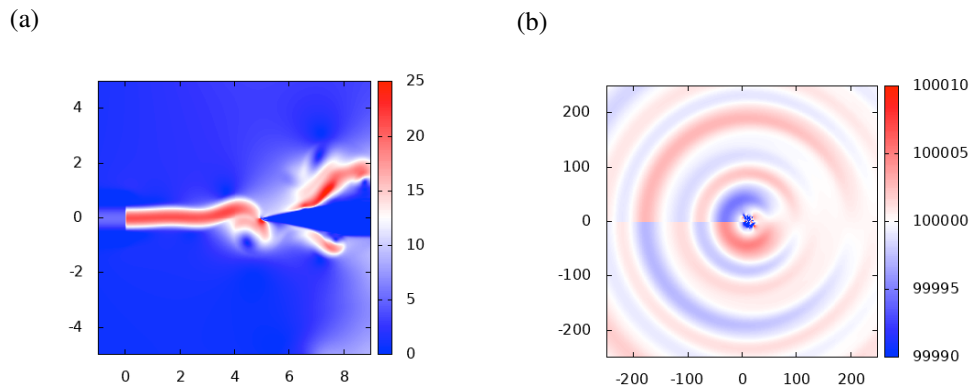


Figure 5. Result of DNS at  $U=18.3\text{m/s}$ . (a) Velocity distribution. (b) Pressure distribution.

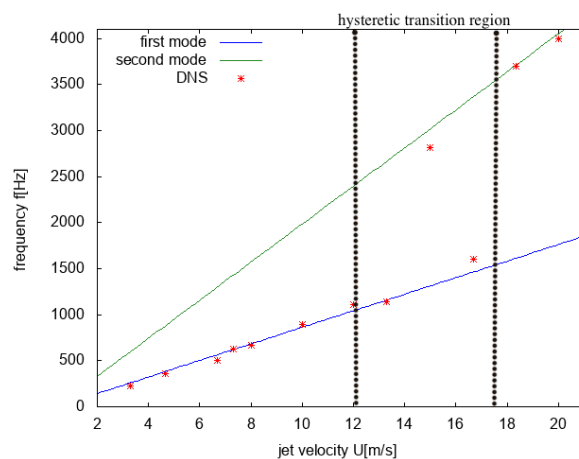


Figure 6. Results of DNS : frequency vs jet velocity. Blue and green lines are first and second modes obtained by Brown's equation (1), respectively. The vertical dotted lines indicate the lower and upper limits of the hysteresis transition region.

## 4.2 LES Results

Calculations with LES are done for the coarse and finer grained meshes. The results for the coarse grained mesh are shown in Figs.7 and 8 and those for the finer grained mesh are shown in Figs.9 and 10. Figure.7 (a) and (b) show velocity and pressure distributions for the coarse grained mesh at  $U = 5.3\text{m/s}$ , respectively. Figure.9 (a) and (b) show those for the finer grained mesh at  $U = 5.3\text{m/s}$ , respectively. For both meshes, hydrodynamic oscillations of the first mode are observed and are very similar to each other. Figure.8 (a) and (b) show velocity and pressure distributions for the coarse grained mesh at  $U = 16.7\text{m/s}$ , respectively. Figure.10 (a) and (b) show those for the finer grained mesh at  $U = 16.7\text{m/s}$ , respectively. As shown in Fig.8, a hydrodynamic oscillation of the first mode is observed for the coarse grained mesh, however as shown in Fig.10 a second mode oscillation is observed for the finer grained mesh. This fact indicates that the coarse grained mesh is insufficient to reproduce the hysteretic mode transition. Note that from the pressure distributions for both coarse and finer grained meshes, an acoustic wave in the upper side and that in the lower side oscillate in anti-phase, which means that the oscillating jet behaves like a dipole source in every case.

Figure.11 shows the change of the sound frequency with the jet velocity  $U$  compared with Brown's equation (1). Below the hysteretic transition region, the calculations for the coarse grained mesh reproduce oscillations of the first mode, however in and above the hysteretic transition region, those for the coarse grained mesh cannot reproduce the appearance of second mode oscillations, which are observed for the calculation with DNS in Fig.6. On the other hands, the finer grained mesh seems to reproduce a second mode oscillation, though its frequency takes a value away from the second mode of Brown's equation (1) and from the results of DNS to a certain extent.

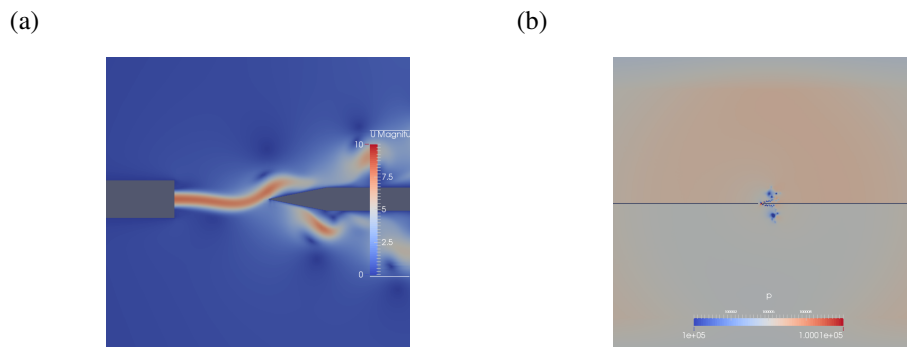


Figure 7. Result of LES at  $U=5.3\text{m/s}$ ,  $\Delta x_{min} = 0.1\text{mm}$ . (a) Velocity distribution. (b) Pressure distribution.

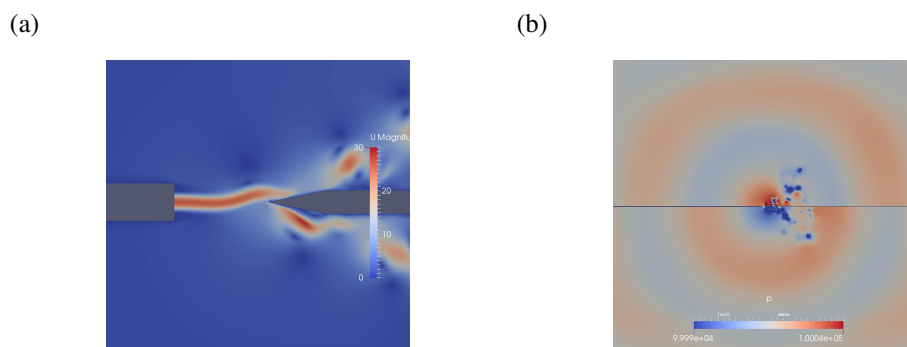


Figure 8. Results of LES at  $U=16.7\text{m/s}$  and  $\Delta x_{min} = 0.1\text{mm}$ . (a) Velocity distribution. (b) Pressure distribution.

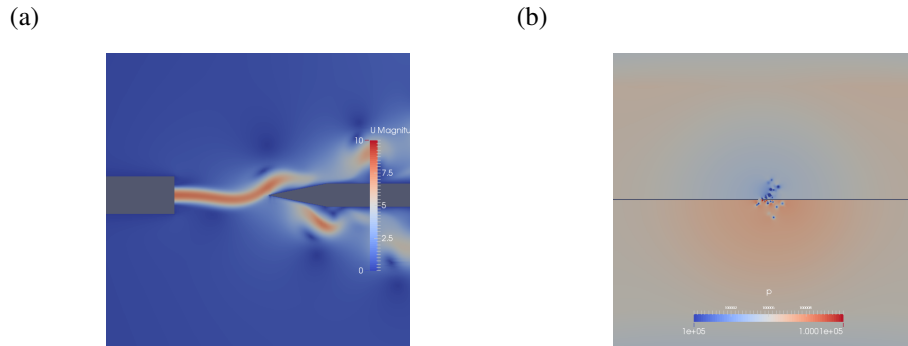


Figure 9. Result of LES at  $U=5.3\text{m/s}$ ,  $\Delta x_{min} = 0.05\text{mm}$ . (a) Velocity distribution. (b) Pressure distribution.

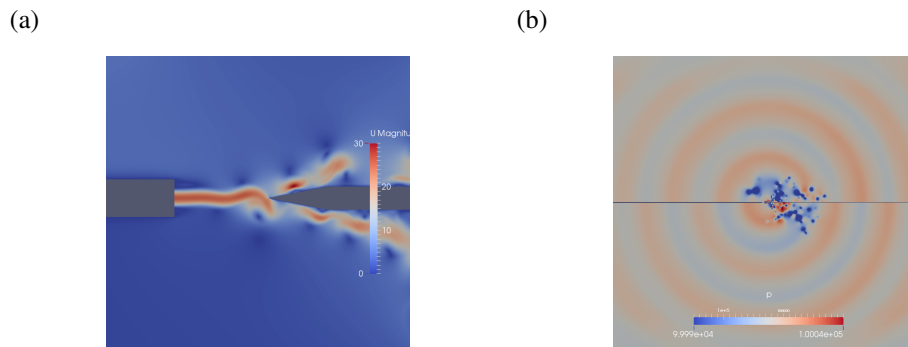


Figure 10. Result of LES at  $U=16.7\text{m/s}$ ,  $\Delta x_{min} = 0.05\text{mm}$ . (a) Velocity distribution. (b) Pressure distribution.

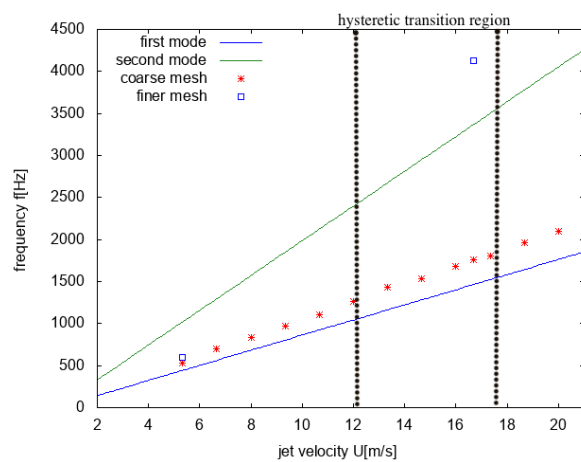


Figure 11. The frequencies obtained with LES for the coarse and finer grained meshes together with the first and second modes of Brown's equation.

## 5 CONCLUSIONS

We confirmed the reliability of the compressible DNS for the calculation of the edge tone. As a result, the hysteretic transition of the edge tone is well reproduced with DNS. Next, we investigated the reliability of the compressible LES taking the compressible DNS as a reference. Below the hysteretic transition region, the calculations with LES taking the coarse grained mesh reproduce oscillations of the first mode, however in and above the hysteretic transition region, those for the coarse grained mesh fail to reproduce the second mode oscillations, though the calculation is not broken down. On the other hands, the calculation with the finer grained mesh seems to reproduce a second mode oscillation, though its frequency takes a value away from the second mode of Brown's equation and from the results of DNS to a certain extent. Therefore, special attention needs to be paid to reproducing the edge tone by using LES. Indeed, it is not break down even though it fails to reproduce the transition when one takes a coarse grained mesh. On the other hand, thank to its accuracy, the compressible DNS should assist one to theoretically investigate the mode transition mechanism of the edge tone.

## ACKNOWLEDGEMENTS

The present work was supported by Grant-in-Aid for Scientific Research (C) Nos. 16K05477 and 19K03655 from the Japan Society for the Promotion of Science (JSPS) and "Joint Usage/Research Center for Interdisciplinary Large-Scale Information Infrastructures" and "High Performance Computing Infrastructure" in Japan (Project IDs: jh180007-MDH and jh190010-MDH). Part of the work was carried out under the Collaborative Research Project of the Institute of Fluid Science, Tohoku University.

## REFERENCES

- [1] M. S. Howe, "*Acoustics of fluid-structure interactions*", Cambridge Univ. Press, Cambridge, 1998.
- [2] N. H. Fletcher and T. D. Rossing, "*The Physics of Musical Instruments*", 2nd Edition, Springer-Verlag, New York, 1998.
- [3] G. B. Brown, "*The vortex motion causing edge tones*", Proc. Phys. Soc., **49** 493 (1937) 493–507.
- [4] A. Powell, "*On the edgetone*", *J. Acoust. Soc. Am.*, **33** (1961) 395–409.
- [5] D. K. Holger, T. A. Wilson, G. S. Beavers "*Fluid mechanics of the edgetone*", *J. Acoust. Soc. Am.*, **62** (1977) 1116–1128.
- [6] D. G. Crighton, "*The jet edge-tone feedback cycle; linear theory for the operating stages*", *J. Fluid Mech.*, **234** (1992) 361–391.
- [7] R. Komatsu, W. Iwakami, Y. Hattori, "*Direct numerical simulation of aeroacoustic sound by volume penalization method*", *Computers and Fluids*, **130** (2016) 24–36.
- [8] C. Wagner, T. Hüttl, and P. Sagaut, eds. "*Large-Eddy Simulation for Acoustics*", Cambridge Univ. Press, New York, 2007.
- [9] M. Miyamoto, Y. Ito, T. Iwasaki, T. Akamura, K. Takahashi, T. Takami, T. Kobayashi, A. Nishida, and M. Aoyagi, "*Numerical study on acoustic oscillations of 2D and 3D flue organ pipe like instruments with compressible LES*", *Acta Acustica united with Acustica*, **99** (2013) 154–171.